In-situ experimental characterization of the clamping pressure effects on low temperature polymer electrolyte membrane electrolysis

Al Shakhshir, Saher; Cui, Xiaoti; Frensch, Steffen Henrik; Kær, Søren Knudsen

Published in:
International Journal of Hydrogen Energy

DOI (link to publication from Publisher):
10.1016/j.ijhydene.2017.07.059

Publication date:
2017

Document Version
Accepted author manuscript, peer reviewed version

In-situ experimental characterization of the clamping pressure effects on low temperature polymer electrolyte membrane electrolysis

Saher Al Shakhshir[*], *Xiaoti Cui, Steffen Frensch, Søren Knudsen Kær*

Department of Energy Technology, Aalborg University, Pontoppidanstr. 111, 9220, Aalborg, Denmark

A B S T R A C T

The recent acceleration in hydrogen production's R&D will lead the energy transition. Low temperature polymer electrolyte membrane electrolysis (LT-PEME) is one of the most promising candidate technologies to produce hydrogen from renewable energy sources, and for synthetic fuel production. LT-PEME splits water into hydrogen and oxygen when the voltage is applied between anode and cathode. Electrical current forces the positively charged ions to migrate to negatively charged cathode through PEM, where hydrogen is produced. Meanwhile, oxygen is produced at the anode side electrode and escapes as a gas with the circulating water.

The effects of clamping pressure (P_c) on the LT-PEME cell performance, polarization resistances, and hydrogen and water crossover through the membrane, and hydrogen and oxygen production rate are studied. A 50 cm^2 active area LT-PEME cell designed and manufactured in house is utilized in this work.

Higher P_c has shown higher cell performance this refers to lower ohmic and activation resistances. Water crossover from anode to cathode is slightly decreased at higher P_c resulting in a slight decrease in hydrogen crossover from cathode to anode. Also, the percentage of hydrogen in the produced oxygen at the anode side is significantly reduced at higher P_c and at lower current density.

Introduction

Hydrogen is considered an important element in direct use for synthetic fuel production, a promising energy carrier, and future replacement for fossil fuel energy sources. Integrating LT-PEME with renewable energy sources makes it one of the most suitable candidate technologies to produce hydrogen directly [1–3]. LT-PEME cells split water into hydrogen and oxygen when an electric potential is applied between anode and cathode. Electrical current forces the hydrogen ions to migrate to negatively charged cathode through the PEM, where hydrogen is produced. Meanwhile, oxygen is produced at the anode side electrode and removed from the cell as a gas with the circulating water. Liquid water and oxygen crossover from anode to cathode and hydrogen crossover in the opposite direction through the membrane takes place at a very small portion compared to the gases production rate on both sides [4].

* *Corresponding author.*
E-mail address: sas@et.aau.dk (S. Al Shakhshir).

Nomenclature

P_c	clamping pressure (psi)
F_c	clamping force (N)
A_c	contact area between the flow field plate and the electrode (m^2)
N	number of bolts (–)
τ	applied torque (N·m)
f	friction coefficient (–)
D	nominal bolt diameter (m)
X_{H_2}	H_2 ratio (–)
X_{O_2}	O_2 ratio (–)
V_{H_2}	H_2 volume flow rate (mlpm)
V_{O_2}	O_2 volume flow rate (mlpm)
V_{N_2}	N_2 volume flow rate (mlpm)
P	membrane permeability coefficient ({(cm^3)(cm)}/{(m^2)(day)(atm)})
D	diffusion coefficient (cm^3s^{-1})
S	solubility coefficient ({cm^3(STP)}/{(cm^3)(atm)})
T	temperature (K)
C	concentration of species (mol·cm^{-3})

Subscripts

i	species
H_2	hydrogen gas
O_2	oxygen gas
N_2	nitrogen gas

Most recent research on LT-PEME has focused on operating conditions such as operating temperature, cathode-anode high differential operating pressure, flow field design, stack development, two-phase flow analysis, precious materials electrocatalyst reduction, low cost and durable PEM and current distributors, scale up of LT-PEME, numerical modeling of complex phenomena taking place inside LT-PEME during operation [5–17]. Also, a lot of studies have been carried out on the effect of clamping pressure on PEM fuel cell characteristics [18–23]. However, the asymmetrical catalysts and electrodes materials on both sides of the LT-PEME: platinum based catalyst with carbon paper/cloth porous transport layer (PTL) electrode on the cathode side and iridium based catalyst with titanium felt (TF) electrode on the anode side, liquid water is used as reactant at the anode side, and the high operating differential pressure between cathode and anode of the LT-PEME. Comparing with symmetrical platinum based catalyst with carbon paper/cloth PTL electrode on both sides, humidified/dry hydrogen reactant at the anode side and humidified oxygen reactant at the cathode side, and zero differential pressure between cathode and anode of PEM fuel cell, respectively. All of these differences might cause different effects of clamping pressure on the LT-PEME than PEM fuel cell. Thus, more experimental and analytical studies of the clamping pressure effect on LT-PEME characteristics are necessary.

Conventional LT-PEME usually clamped with bolts around the active area. Thus, P_c can be calculated from clamping force (F_c) applied on the cell divided by the contact area given by:

$$P_c = \frac{F_c}{A_c} \tag{1}$$

Stainless steels bolts are commonly used to compress the cell components against each other as shown in Fig. 1.

Thus F_c can be given by Ref. [24]:

$$F_c = \frac{N \times \tau}{f \times D} \tag{2}$$

where N is the number of bolts distributed symmetrically around the active area of the membrane, τ is the applied torque on each bolt (N·m), f is the friction coefficient (0.2 for steel bolts), and D is the nominal bolt diameter (m). It should be borne in mind that A_c has different dimensions by different researchers in PEM fuel cell which are considered very similar to LT-PEME cell. Hassan et al. [25] defined it as the active area of the membrane, Ahmad et al. [18] defined it as the PTL and the sealing gasket surface area, and Mehboob et al. [24] referred to it as the total contact area between bipolar plate and end plate. These different definitions of A_c might lead to inaccurate calculations of P_c from F_c. Furthermore, the ribbed design of the flow field is another source of error, because the area of the ribs is the only area that compresses against the electrodes, and this makes A_c less than the membrane active area. Thus, to be more accurate, A_c can be defined as the contact area between the flow field plate and the electrode.

Small efforts were made to study the effect of P_c on the LT-PEME characteristics. Siracusano et al. [26] concluded that, a modest enhancement in the 3-cells stack performance was observed at higher compression due to better electrode-electrolyte interface especially at the cathode side. Meanwhile, no significant modifications were noticed on the polarization curves for each cell in the 3-cell stack, and a slight improvement in polarization resistances at higher compression was observed. As shown earlier, the compression force is directly related to the applied torque on each bolt in bolted LT-PEME cell. Selamet et al. [27,28] studied the effect of bolt torque on LT-PEME cell performance, durability, and contact resistant. They found that, the optimized applied bolt torque is important for homogeneous water distribution and consequently higher durability, performance, and lower contact

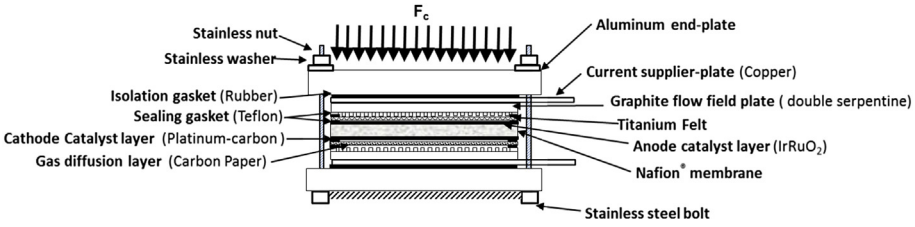

Fig. 1 – Schematic of LT-PEME cell compressed with stainless steel bolts.

resistant. They also, concluded that, increasing the bolt torque of a single LT-PEME cell at 0.5 Acm^{-2} and ambient temperature results in more contact points between cell layers and consequently the contact resistant was reduced and the cell performance was developed. However, beyond a certain torque the performance starts to decrease due to the mass transport limitation [29]. Awsthi et al. [30] dynamically modeled LT-PEME system under a wide range of operating conditions; they found that, increasing the compression pressure decreases the cell performance. This because, in their model increasing the cell pressure resulted in increasing the partial pressure of the species which in turn increase the open circuit voltage calculated by Nernst equation. This agrees with Marangio et al. [31] who concluded that, the kinetic of the charge transfer could be reduced at higher counter pressure resulting in higher cell polarization. Furthermore, the asymmetrical components on the two sides of the LT-PEME might lead to un-equal compression force on both sides of the membrane due to the difference in the mechanical properties such as elastic and plastic deformation for both electrodes, and the TF pores and fibers diameters are larger and much harder than the PTL pores and fibers diameters. Thus, inhomogeneous compression against the TF might damage the catalyst layer by sinking the TF fibers in the catalyst layer at the anode side [5].

Therefore, the effects of P_c on the LT-PEME on cell performance, ohmic and activation resistances, water, oxygen, and hydrogen crossover rates through the membrane, and hydrogen and oxygen production rates at different current densities are in-situ experimentally demonstrated in this work. A 50 cm^2 single LT-PEME cell is utilized, and all the measurements are conducted in real time at 70 °C and atmospheric pressure. Furthermore, to avoid inhomogeneous P_c by bolting the cell around the active area, a precise compression set-up uses plate like piston which is in contact with the whole surface of the end plate resulting in uniform compression pressure on the end plate surface and maybe on the active area as well, hence all LT-PEME cell layers are aligned with each other.

Experimental

Experimental test-rig

A LT-PEME single cell test-rig was assembled and integrated in-house from different equipment for in-situ testing of single LT-PEME cell as shown in Fig. 2.

The single cell test-rig consists of a deionized (DI) water supply, water heater, heat exchanger, centrifugal pump, flow meters, thermocouples, pressure gauges, water tank, liquid drainer, water scale and gas analyzer. The DI water system components, water drainer, and the water scale are part of a fuel cell automated test station FCATS G60 (Greenlight Innovation) used to control the water and cell temperature, separate the water from hydrogen, and to weight the condensed water, respectively. The gas analyzer (SIEMENS ULTRAMAT 23 for O_2 and CALOMAT 6 for H_2) is used to analyze and measure

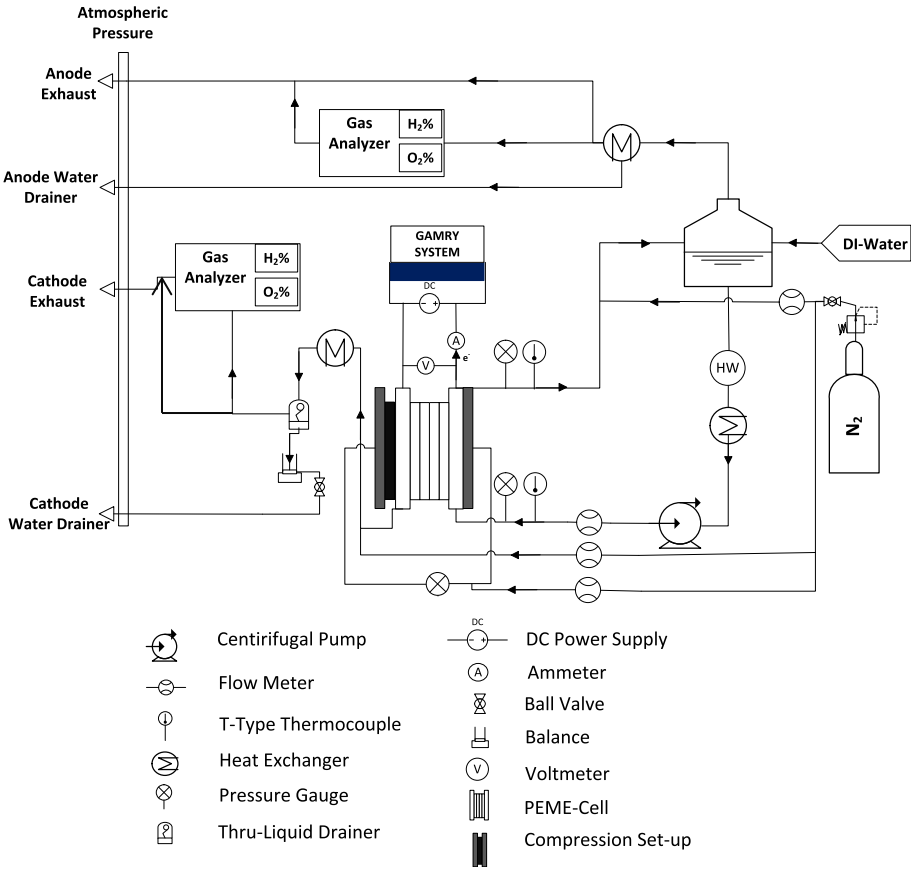

Fig. 2 – Schematic of LT-PEME single cell's test-rig.

the gas production rates for the anode and cathode gases. Also, the gas analyzer was always working in a vacuum mode (1.0 lpm) and all the atmospheric exhausts were under vacuum mode to prevent any air to enter from the atmosphere to the system.

The Gamry Reference 3000 device (Gamry Instruments, Inc.) integrated with FCATS was used to carry out the impedance measurement of the LT-PEME. An external High Power Bipolar Power Supply (KEPCO BOP 10-75MG) controlled digitally by General Purpose Interface Bus (GPIB) was used to supply the cell with the current. The KEPCO BOP model is a 4-quadrant programmable voltage and current power supply which allow both power sourcing and sinking. The power supply can also measure the current and the voltage while it is supplying the cell with current. This allows the polarization curve to be constructed without using any extra voltmeter or ammeter. Furthermore, to minimize the induction noise, all the sensing cables for the power supply and the Gamry system were shielded.

The compression set-up made by TP50 Research Cell components (Tandem Technologies Ltd) was used to clamp the LT-PEME cell directly from the whole area of the end plate at a certain P_c. The P_c value can be controlled by the nitrogen flow from the nitrogen cylinder, and this can be performed while the cell is running. On the other hand, the pressure of the water-oxygen at the anode outlet and the hydrogen-water at the cathode outlet were kept at atmospheric pressure.

LT-PEME single cell

A 50 cm^2 LT-PEME cell was assembled as shown in Fig. 1. TF with fiber diameter of 20 μm, a weight of 300 g/cm^2, a porosity of 81% and a thickness of 0.35 mm [11]. Meanwhile, the PTL (AvCarb P75) made from carbon paper substrate with 245 microns thickness and 0.0075 g/cm^2. Current distributor plates were made from copper with 3 mm thickness and the end-plates were made from aluminum with 20 mm thickness. The flow field plates were made from 3 mm graphite composites plates, and they were machined in-house with 1 × 1 mm channel cross section, and with double serpentine flow field layout.

A commercial MEA with anode and cathode electro catalyst consists of 3 mg/cm^2 Iridium Ruthenium Oxide and 3 mg/cm^2 Platinum Black, respectively. The catalyst materials were sprayed on a Nafion® 115 membrane with 127 μm thickness. Also, the cell was sealed with Teflon gasket with 0.35 mm and 0.25 mm thickness at the anode and cathode side, respectively, and the end plates were isolated from the current distribution plate with 0.2 mm Teflon gasket on both sides of the LT-PEME cell.

Experimental conditions, procedures, and uncertainties

Testing procedures

Before starting the experiment, the membrane was humidified by circulating the preheated DI-water through the anode side. The cell temperature was controlled by the water temperature. When the cell temperature reached 70 °C the current was supplied to the cell. Meanwhile, when the cell was running at high current densities, the temperature of the LT-PEME cell measured at the cathode and anode flow field plate and the water and oxygen stream escaping the LT-PEME cell increased above 70 °C, thus the temperature of the water at the inlet is controlled accordingly to keep the cell temperature and the oxygen and water stream at the cell outlet constant at 70 °C.

After the cell reached steady state, the following data were collected with 0.5 Hz frequency over 10 min period of time: Voltage and current, hydrogen crossover rate from cathode to anode, O_2 production rate, and H_2 production rate. The gases measurements were performed by analyzing the outlet gas streams for anode and cathode. All of these measurements were carried out at different current densities (0.1–1.3) A/cm^2 with 0.4 A/cm^2 step value. The steady state time was 30 min until the cell temperature and the voltage value are stabilized at fixed current density. The impedance measurement was performed also after reaching the steady state and the test was initiated at 10 kHz and stopped automatically at 1.0 mHz. For water crossover rate measurements, the water was collected for a 30 min period after reaching the steady state. The 30 min period allows the collection of enough amount of water for precise weighting and the water crossover rate as converted to mg/s.

After connecting the LT-PEME cell a simple test for hydrogen leak was performed using a hydrogen sensor. The leak stopped when P_c reached 50 psi. Also, any water leak was stopped at the same pressure. Thus, the lower P_c value starts from 60 psi and due to the limitation of TP50 compression setup, the higher value ends at 150 psi. These values can be converted to bolt torque assuming the cell is bolted with 8 bolts as: 5, and 13 Nm, respectively. This torque values are comparable with Selamet et al. [29] applied torque range. After making sure that the cell was working properly, the experiments were started and all the experiments were fully automated and controlled with LabVIEW software and remotely accessed.

Experimental conditions

The LT-PEME cell was experimentally conditioned according the described experimental conditions in Table 1.

Experimental uncertainty

All the used equipment has high measuring accuracy as illustrated in Table 2.

Table 1 – Experimental conditions for in-situ LT-PEME cell testing.

Description	Value
DI-water temperature, T (°C)	70
Working pressure (atm)	1
DI-water flow rate (mlpm)	100
Clamping pressure (psi)	60, 150
LT-PEME cell temperature T (°C)	70
Data collecting frequency (Hz)	0.5
Data collecting time (min)	30
Steady state time (min)	30
Gas analysis temperature T (°C)	140
Gas analysis flow rate (lpm)	1
Impedance frequency (initial –final) (Hz)	10,000–0.01
Perturbation AC-current (A)	2.5% of the supplied DC current

As highlighted in our previous work, the standard error could not be calculated directly using a mathematical formula. Thus the confidence level from the generated experimental data was estimated by calculating the coefficient of variation from the repeated experiments for few times at certain conditions [32].

Gas analysis

The gases were analyzed and measured using the SIEMENS gas analyzer (ULTRAMAT 23 CALOMAT 6). A cooler (M&C EC cooler) is integrated with in the gas analyzer to get rid of moisture in the stream before it is analyzed by the gas analyzer sensors. The gas analyzer is also equipped with a vacuum pump, conditioned to run the gas stream entering the gas analyzer at 1.0 lpm. Thus the product gases (H_2 and O_2) were mixed with 1.0 lpm nitrogen before entering the gas analyzer to ensure that the total flow rate of the gas mixture is always more than 1.0 lpm, and the excess flow is exhausted as shown in Fig. 2.

The gas analyzer measures the ratio (X) of oxygen and hydrogen in the stream and the rest is nitrogen as given by the following equations;

$$X_{H_2} = \frac{V_{H_2}}{V_{H_2} + V_{O_2} + V_{N_2}} \tag{3}$$

$$X_{O_2} = \frac{V_{O_2}}{V_{H_2} + V_{O_2} + V_{N_2}} \tag{4}$$

where X is the measured ratio and V is the volumetric flow rate (V_{N_2} = 1.0 lpm). Solving these two equations with two unknowns; V_{H_2} and V_{O_2}, yields;

$$V_{H_2} = \frac{V_{N_2} + V_{N_2}\left(\frac{1}{X_{O_2}} - 1\right)}{\left(\frac{1}{X_{H_2}} - 1\right)\left(\frac{1}{X_{O_2}} - 1\right) - 1} \tag{5}$$

Then, V_{O_2} can be calculated by substituting V_{H_2} in Eq. (3) or (4).

Results & discussion

Effect of clamping pressure on the polarization resistances

The clamping pressure has a direct and significant effect on the ohmic, activation, and concentration resistances as seen in Fig. 3. Also, the voltage at 150 psi is lower than the voltage at 60 psi at the same current density, and this can be referred as a better cell performance [33].

The ohmic and activation resistances are higher at lower P_c. This is due to lower cell conductivity and higher kinetic resistance for driving the reaction. The impedance measurements showed lower ohmic and activation resistance at higher P_c as shown in Fig. 4.

As noticed in Fig. 4, the effect of P_c on the ohmic and activation resistance is very obvious from the first. Both resistances decrease with increasing P_c due to the reduction in contact and interfacial resistances at higher P_c. Also, the concentration polarization might be increased due to high reaction rate which requires more water to be transported to the reaction sites at higher current densities. Meanwhile, the smaller pores of the TF at higher P_c might reduce the amount of water transported to the reaction sites. Despite the fact that the concentration polarization might increase at higher P_c and higher current densities, the cell performance is still higher at higher P_c and higher current densities. This suggests that the ohmic resistance effect on the LT-PEME cell performance is more dominant and this agrees with Awasthi et al. [30]. In other words, the ohmic resistance was reduced significantly at higher P_c at the same current density and it was slightly increased at higher current densities and the same P_c as discussed in our previous work [32].

Effect of clamping pressure on the gas crossover and generation rate

The effect of gas crossover rate on the overall cell performance, durability, and membrane degradation are thoroughly investigated for PEM fuel cells [34–37]. Furthermore, Laconti et al. [38] studied the gas crossover phenomena in LT-PEME. They found that increasing the water content in the PEM dissolve more gases resulting in higher gas crossover rate. Also, they concluded that the diffusion mechanism is the only driver mechanism for the gas crossover through the membrane.

In PEM fuel cell, increasing the clamping pressure and the current density increases the hydrogen crossover rate through the membrane [39]. Meanwhile, the P_c has shown an opposite

Table 2 – Measuring Accuracy of the test set-up equipment.

Description	Accuracy
Gas analyzer	<1% of measuring scale
Voltage measurement (V)	0.05% of the read value
Current measurement (A)	0.1% of the read value
Impedance measurement (Ω)	1% of the read value
DI-water flow measurement (lpm)	1% of the reading
DI-water temperature measurement (°C)	±0.5
DI-water pressure measurement (kPa)	±2 (0.5% FS[a])
End-plate temperature measurement (°C)	±0.5

[a] FS: full scale.

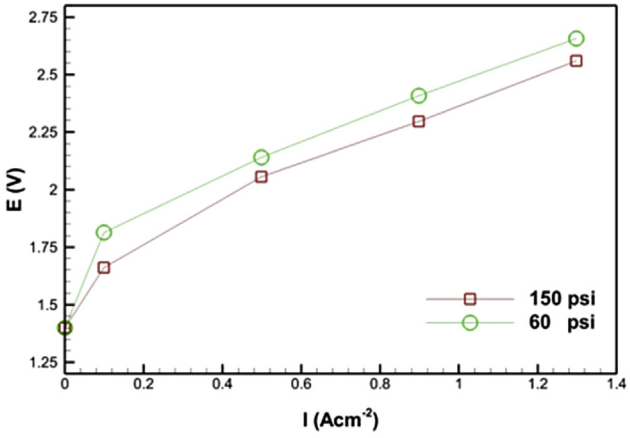

Fig. 3 – Polarization curve at different P_c, 70 °C cell temperature, and atmospheric pressure.

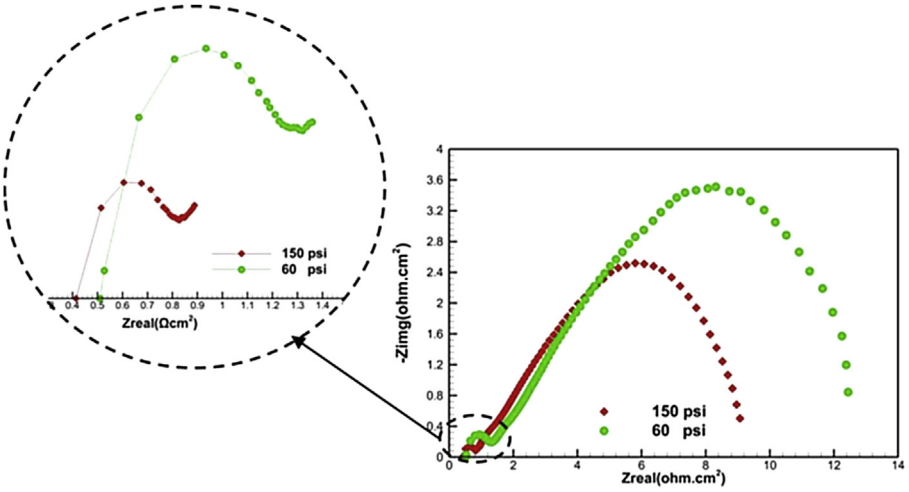

Fig. 4 – Impedance measurements plot zoomed-in on the left of the figure at different P_c and 0.1 Acm^{-2}, 70 °C, and atmospheric pressure.

effect on the hydrogen crossover in LT-PEME as illustrated in Fig. 5.

As noticed in Fig. 5, higher P_c has shown a slightly lower hydrogen crossover rate at the same current density. Meanwhile, Jung et al. [39] has shown opposite behavior in PEM fuel cell. In other words, increasing P_c in PEM fuel cell increases the hydrogen crossover rate slightly due to higher membrane swelling. It should be borne in mind that in PEM fuel cell reactants are humidified hydrogen and humidified air at the anode and cathode side, respectively. Meanwhile, liquid DI-water is the only reactant at the anode side of LT-PEME. Thus, the effect of P_c on the hydrogen crossover rate in LT-PEME may not be similar to the effect of P_c in PEM fuel cell.

The effect of the P_c on hydrogen crossover rate in LT-PEME can be elucidated to the water content in the membrane at different clamping pressures. Water crossover rate from anode to cathode can be used as an indicator for the water content in LT-PEME; higher water crossover rate means higher membrane's water content and lower water crossover rate indicates lower membrane's water content. Thus, the water crossover rate was measured in this work as shown in Fig. 6.

As noticed in Fig. 6, water crossover rate from anode to cathode of LT-PEME at 60 psi is slightly higher than at 150 psi. This means at 60 psi water content in the membrane is higher, thus the hydrogen crossover rate at the same current density is slightly higher at lower P_c. This might be elucidated to the smaller pore sizes of the TF and the membrane as a result of increasing the total pressure on the TF from 60 to 150 psi. It should be borne in mind that, Olesen et al. [11] have concluded that, the pore size of the TF decreases linearly with increasing the applied pressure. Smaller TF pore size might result in less liquid water transport through the TF and diffusion through the membrane from anode to cathode. Also, the amount of produced hydrogen at different P_c might affect the hydrogen crossover rate as shown in Fig. 7.

As noticed in Fig. 7, hydrogen production rate at the LT-PEME cathode side is slightly lower at higher P_c. This might be attributed to the lower amount of transported water to the anode catalyst layer due to the smaller pores of the TF at higher P_c as shown in Fig. 6. Hence, both sides of LT-PEME

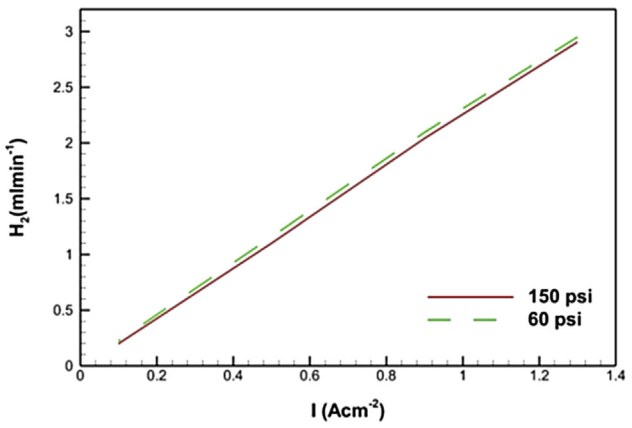

Fig. 5 – Hydrogen crossover rate from cathode to anode at different P_c, 70 °C cell temperature, and atmospheric pressure.

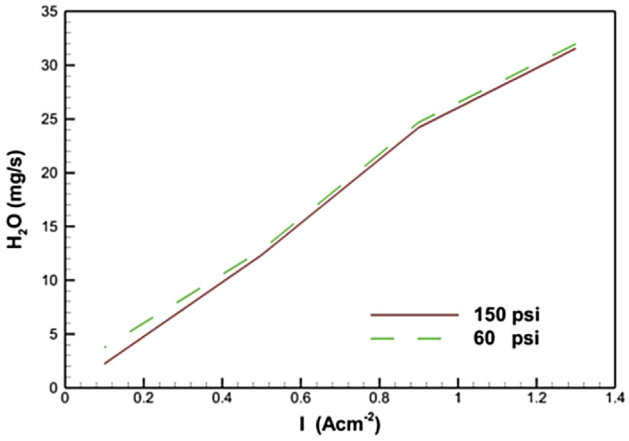

Fig. 6 – Water crossover rate from anode to cathode at different P_c, 70 °C cell temperature, and atmospheric pressure.

operated at the same pressure (1 atm), a slight increase in the amount of produced hydrogen at the same current density might lead to the slight increment in hydrogen crossover rate as shown in Fig. 5. Also, lower hydrogen production at higher P_c results in lower Faraday efficiency. This does not agree with Siracuaano et al. [26] who concluded that, Faraday efficiency for 3-PEME cell stack increased with increasing P_c due to less hydrogen leakage at higher P_c whereas, the hydrogen leak in this work was almost 0 ppm. Hence, the test will automatically shut down if there is any hydrogen leakage even on the level of few ppms.

It should be borne in mind that the percentage of hydrogen crossover rate with respect to hydrogen production rate is increasing with increasing the current density as shown in Fig. 8.

As depicted in Fig. 8, the effect of P_c on the ratio of crossover rate of H_2 to the production rate of H_2 is more dominant at low current density. This is attributed to the low amount of H_2O dragged by H^+ passing through the membrane resulting in lower water content in the membrane at lower current density and consequently lower amount of hydrogen production and crossover rates. Despite the fact that P_c has a slight effect on the hydrogen crossover rate, the current density has a significant effect on the hydrogen crossover rate as depicted in Figs. 5 and 8. The relationship between the current density and the hydrogen crossover rate is directly proportional relationship and this agrees with Bessarabov et al. [40]. This is elucidated to higher amount of charge H^+ passing through the membrane at higher current density due to electro-osmotic drag resulting in dragging more H_2O and this increases the water content in the membrane resulting in the higher rate of water crossover rate from anode to cathode as depicted in Fig. 6. Increasing the water content in the membrane increases the amount of hydrogen dissolved in the water resulting in higher hydrogen crossover rate from cathode to anode at higher current densities as noticed in Fig. 5. This also agrees with the definition of gas permeability coefficient through the Nafion membrane as a product of diffusion and solubility coefficients given by Ref. [41]:

$$P = D \times S \tag{6}$$

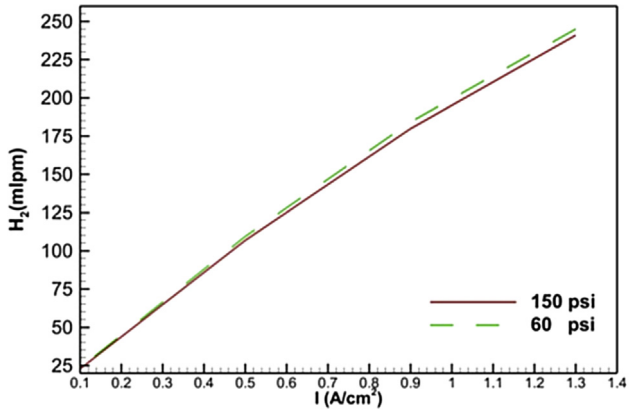

Fig. 7 – Hydrogen production rate at the cathode side at different P_c, 70 °C cell temperature, and atmospheric pressure.

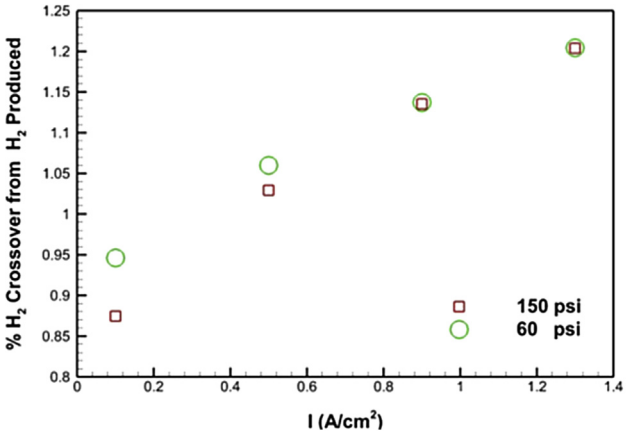

Fig. 8 – Ratio of H_2 crossover rate to hydrogen production rate vs. current density at different P_c, 70 °C cell temperature, and atmospheric pressure.

where P, D, and S are the permeability ({(cm^3)(cm)}/{(m^2)(day)(atm)}), diffusion (cm^3/s), and solubility ({cm^3(STP)}/{(cm^3)(atm)}) coefficients, respectively. STP is the standard conditions for temperature and pressure at 20 °C and 1 atm.

The LT-PEME cell hydrogen crossover rate might not be changed significantly at different P_c especially at higher current densities. However, changing the operating temperature of the same LT-PEME cell has shown more significant effect on the hydrogen crossover rate from cathode to anode for the same LT-PEME cell as shown in Fig. 9.

As noticed in Fig. 9, hydrogen crossover rate is more sensitive to the temperature change than P_c change as depicted in Fig. 5. This is because the permeability of the gases through the membrane is directly related to the diffusion coefficient and temperature as given by Ref. [42]:

$$D_i = P_i^m RTC_i \tag{7}$$

where P^m is the gas permeability, R is the constant of ideal gas: 8314×10^6 Pa cm^3·K^{-1} mol^{-1}; T is the temperature in K; C_i is the concentration of species i in mol·cm^{-3}.

As noticed in Fig. 10, the P_c has almost no effect on the amount of generated oxygen at the anode side. At higher cell performance, the amount of electric current fed to the LT-PEME is less as shown in Fig. 3, but still the cell gives almost the same amount of oxygen and a slightly less amount hydrogen as noticed in Fig. 7. In other words, increasing P_c at the same current density and the same anode and cathode operating pressure reduces the hydrogen crossover rate resulting in higher cell performance and lower degradation rates. This is because, the PEM degradation rate is directly related to gases crossover through the membrane and their catalytic combustion [43]. Also, the gases crossover through PEM can cause a parasitic power loss and this might affect the long term performance [38].

The effect of P_c can be noticed on the ratio of H_2 in O_2 at the anode side as shown in Fig. 11.

The ratio of H_2 in O_2 at the anode side is reduced at higher P_c value. This is due to higher H_2 crossover rate at lower P_c value as mentioned earlier. Also, higher ratios of H_2 in O_2 in the LT-PEME anode side are more noticeable at lower current

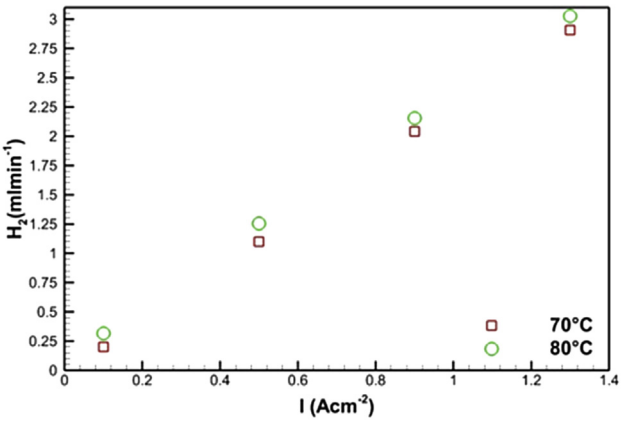

Fig. 9 – Hydrogen crossover at different temperatures, P_c = 150 psi, and atmospheric pressure.

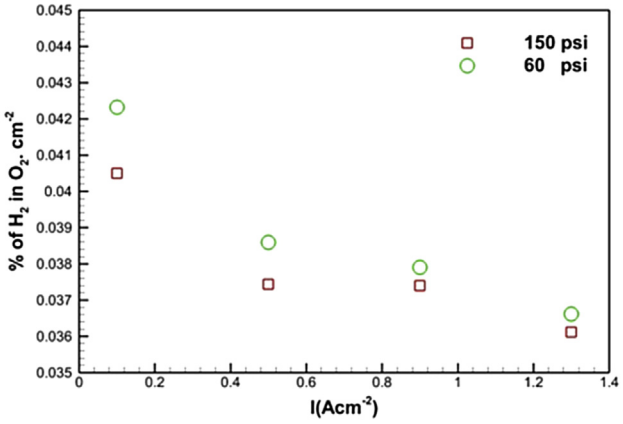

Fig. 11 – Ratio of H_2 in O_2 at different P_c, 70 °C cell temperature, and atmospheric pressure.

densities as depicted in Fig. 11. Despite the fact that the LT-PEME cell was operated at atmospheric pressure on both sides of the membrane, the ratio of H_2 in O_2 at the anode side is still higher at lower current densities and lower P_c. This is due to the lower amount of produced oxygen and relatively higher hydrogen crossover rate. This suggests that, running the LT-PEME cell at higher cathode pressure results in much higher ratios of H_2 in O_2 in the anode side at lower current densities and lower P_c. Thus, safety parameters should be considered to avoid higher ratio of H_2 in O_2 at the anode side to avoid reaching the explosion point.

The small size of hydrogen molecules makes it more mobile in the LT-PEME cell than the oxygen molecules. This leads to higher hydrogen crossover rate than oxygen crossover rate. Thus, it is always essential to evaluate the ratio of H_2 in O_2 at the anode side of LT-PEME as mentioned earlier to avoid higher ratio of H_2 in O_2 where the explosion point might be reached. Meanwhile, the larger size and molecular weight of an O_2 molecule makes it less mobile with lower crossover rate through the membrane from anode to cathode side [44]. Thus, evaluating the ratio of O_2 in H_2 in the cathode side is helpful for estimating the corrosion rate for cathode side components. Bessarabov et al. [40] measured the ratio of O_2 in H_2 at 50 °C as 0.001% and 0.00103% O_2 in $H_2 \cdot cm^{-2}$ at 0.25 and 0.5 Acm^{-2}, respectively. These values are close to 0.0% and 30 times less than the percentage of H_2 in O_2 measured in this work. Thus, it is very hard to measure the percentage of O_2 in H_2 by means of the formerly used equipment. This is because the ULTRAMAT 23 accuracy level is around 0.02% O_2 in $H_2 \cdot cm^{-2}$. Thus, the percentage of O_2 in H_2 is assumed to be very close 0.0% in this work.

The level of confidence in the measured data was calculated from the repeated experiments for hydrogen and water crossover rate, O_2 production rate, and measured voltage. All the measurements were repeated for 10 times as shown in Fig. 12.

It is noticed that the hydrogen crossover rate, oxygen production rate, and voltage data have shown more than 98% confidence level. This is due to the high accuracy of the used equipment. On the other hand, the water crossover rate measurement has shown above 95% confidence level at 0.2 Acm^{-2} and above 96% confidence level for the rest of the current densities. The water at the cathode side outlet was collected for 30 min period as mentioned earlier after the LT-PEME reached the steady state. The lower confidence level in

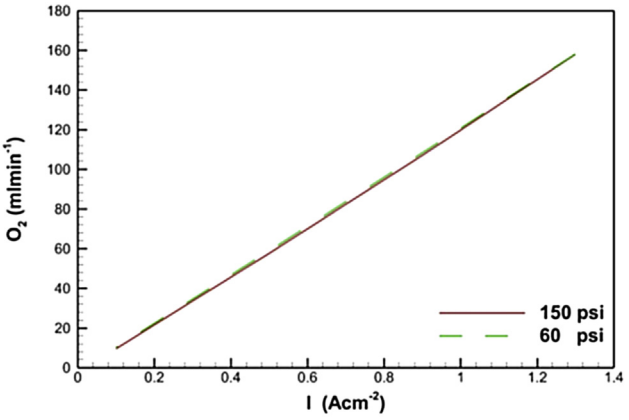

Fig. 10 – Oxygen production rate at the anode side at different P_c, 70 °C cell temperature, and atmospheric pressure.

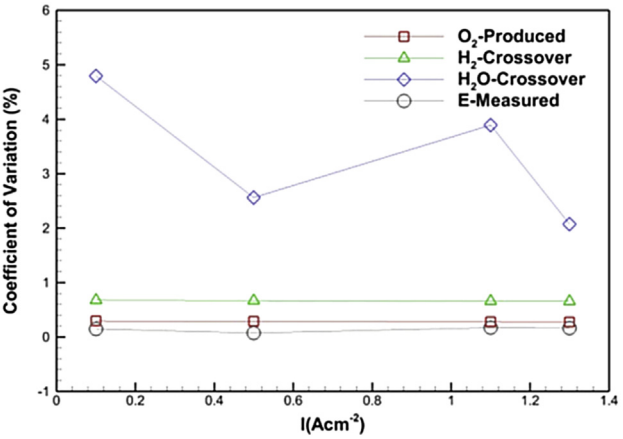

Fig. 12 – Confidence level of the measured hydrogen and water crossover, produced O_2, and measured voltage at P_c = 150 psi, 70 °C, and atmospheric pressure.

water collection measurements was expected especially at low current densities. This is because the water has to be condensed in the heat exchanger first, after that the hydrogen is separated from the water by the thru-liquid drainer and then the water is weighted by the balance as shown in Fig. 2. It should furthermore be borne in mind that the hydrogen stream might still carry a small amount of water with it after passing through all of these processes. However, all water crossover measurements were measured using the same technique as shown in Fig. 2. Thus, the measurements of water crossover rate at different current densities and P_c are comparable with each other.

Conclusion

In this work, the effect of clamping pressure on the LT-PEME cell's characteristics was experimentally demonstrated using real time in-situ measurements. The effect of the clamping pressure can be summarized as the following:

- Increasing the clamping pressure from 60 to 150 psi increased the LT-PEME cell's performance. This is attributed to reduction of the ohmic and activation resistance at higher clamping pressure. The contact resistance between the cell components and the charge transfer-kinetics for the oxygen and hydrogen evolution reactions rates at the electrode surfaces are suspected to be reduced at higher clamping pressure. Thus, the cell performance increases at higher clamping pressure.
- The reduction in ohmic and activation resistances can be noticed at low and high current densities with increasing the clamping pressure. However, at the same clamping pressure, the ohmic resistances are almost the same at low and high current density. Meanwhile, the activation resistances are significantly decreased at higher current density. This can be elucidated to the small amount of electrons present at low current density and this means a larger resistance is required to drive the reaction.
- Despite the fact that the concentration over potential might be increased at higher current densities and higher clamping pressure, the cell performance is still higher at higher clamping pressure. This suggests that the ohmic resistance is more dominant in affecting the cell performance.
- Hydrogen crossover rate is slightly reduced at higher clamping pressure. This is attributed to the lower membrane swelling. Higher clamping pressure leads to the reduction in the pore size of TF and membrane pores. Thus, less water is transported to the reaction sites through the TF and less water diffuses through the membrane. This results in less water crossover rate to cathode side and slightly less hydrogen production rate and consequently less hydrogen crossover rate to anode side. It should be borne in mind that lower hydrogen crossover rate means less percentage of H_2 in O_2 at the cathode side, which is important to avoid explosion. Also, it might lead to slower degradation rate of LT-PEME.
- LT-PEME current density has shown more significant effect on hydrogen crossover rate than the clamping pressure. This is because at higher current densities more H_2O molecules dragged by H^+ through the membrane due to electro-osmotic drag. This will increase the membrane water content resulting in more hydrogen solubility in H_2O. Thus, hydrogen crossover rate and water crossover rate increases significantly at higher current densities.
- Despite the fact that the operating pressure on both sides of the membrane is atmospheric pressure in this work, the hydrogen ratio in oxygen at the anode side of LT-PEME is noticeably increased with decreasing the clamping pressure at lower current densities. This is due to higher hydrogen crossover rate at lower clamping pressure and lower oxygen production rate at lower current densities. Thus, more safety precaution has to be taken especially when running the cell at higher cathode pressure.
- LT-PEME temperature has more significant effect on the hydrogen crossover rate than the clamping pressure. This is because the gas diffusion coefficient in the Nafion membrane is directly related to the membrane temperature.

Overall, the effect of the clamping pressure on the LT-PEME cell characteristics is experimentally demonstrated in this work. Currently, work is still in progress to study the effect of clamping pressure on LT-PEME degradation and to perform more analytical studies on the LT-PEME clamping pressure.

Acknowledgements

The authors would like to acknowledge the supported of this work from the Danish ForskEL program through the Power2-Hydrogen project, Grant 12.313 and Innovation Fund Denmark through the e-STORE project, Grant 4106-00025B.

REFERENCES

[1] Becker S, Karri V. Predictive models for PEM-electrolyzer performance using adaptive neuro-fuzzy inference systems. Int J Hydrogen Energy 2010;35(18):9963–72.
[2] Clark WW. The green hydrogen paradigm shift. Cogener Distrib Gen J 2007;22(2):6–38.
[3] Maclay JD, Brouwer J, Samuelsen GS. Dynamic modeling of hybrid energy storage systems coupled to photovoltaic generation in residential applications. J Power Sources 2007;163(2):916–25.
[4] Onda K, Kyakuno T, Hattori K, Ito K. Prediction of production power for high-pressure hydrogen by high-pressure water electrolysis. J Power Sources 2004;132(1):64–70.
[5] Bessarabov D, Wang H, Li H, Zhao N. PEM electrolysis for hydrogen production: principles and applications. CRC Press; 2015.
[6] Grigoriev SA, Millet P, Volobuev SA, Fateev VN. Optimization of porous current collectors for PEM water electrolysers. Int J Hydrogen Energy 2009;34(11):4968–73.
[7] Helm ML, Stewart MP, Bullock RM, DuBois MR, DuBois DL. A synthetic nickel electrocatalyst with a turnover frequency above 100,000 s−1 for H_2 production. Science 2011;333(6044):863–6.
[8] Lafmejani SS, Olesen AC, Kær SK. Analysing gas-liquid flow in PEM electrolyser micro-channels. ECS Trans 2016;75(14):1121–7.
[9] Millet P, Dragoe D, Grigoriev S, Fateev V, Etievant C. GenHyPEM: a research program on PEM water electrolysis

supported by the European Commission. Int J Hydrogen Energy 2009;34(11):4974–82.
[10] Nie J, Chen Y. Numerical modeling of three-dimensional two-phase gas–liquid flow in the flow field plate of a PEM electrolysis cell. Int J Hydrogen Energy 2010;35(8):3183–97.
[11] Olesen AC, Rømer C, Kær SK. A numerical study of the gas-liquid, two-phase flow maldistribution in the anode of a high pressure PEM water electrolysis cell. Int J Hydrogen Energy 2016;41(1):52–68.
[12] Onda K, Murakami T, Hikosaka T, Kobayashi M, Ito K. Performance analysis of polymer-electrolyte water electrolysis cell at a small-unit test cell and performance prediction of large stacked cell. J Electrochem Soc 2002;149(8):A1069–78.
[13] Van der Merwe J, Uren K, Van Schoor G, Bessarabov D. Characterisation tools development for PEM electrolysers. Int J Hydrogen Energy 2014;39(26):14212–21.
[14] Wei G, Xu L, Huang C, Wang Y. SPE water electrolysis with SPEEK/PES blend membrane. Int J Hydrogen Energy 2010;35(15):7778–83.
[15] Zhang H, Su S, Lin G, Chen J. Efficiency calculation and configuration design of a PEM electrolyzer system for hydrogen production. Int J Electrochem Sci 2012;7(4):4143–57.
[16] Yigit T, Selamet OF. Mathematical modeling and dynamic Simulink simulation of high-pressure PEM electrolyzer system. Int J Hydrogen Energy 2016;41(32):13901–14.
[17] Lee B, Park K, Kim H-M. Dynamic simulation of PEM water electrolysis and comparison with experiments. Int J Electrochem Sci 2013;8:235–48.
[18] Ahmed DH, Sung HJ, Bae J. Effect of GDL permeability on water and thermal management in PEMFCs—II. Clamping force. Int J Hydrogen Energy 2008;33(14):3786–800.
[19] Asghari S, Mokmeli A, Samavati M. Study of PEM fuel cell performance by electrochemical impedance spectroscopy. Int J Hydrogen Energy 2010;35(17):9283–90.
[20] Bates A, Mukherjee S, Hwang S, Lee SC, Kwon O, Choi GH, et al. Simulation and experimental analysis of the clamping pressure distribution in a PEM fuel cell stack. Int J Hydrogen Energy 2013;38(15):6481–93.
[21] Lee WK, Ho CH, Van Zee JW, Murthy M. The effects of compression and gas diffusion layers on the performance of a PEM fuel cell. J Power Sources 1999;84(1):45–51.
[22] Wang X, Song Y, Zhang B. Experimental study on clamping pressure distribution in PEM fuel cells. J Power Sources 2008;179(1):305–9.
[23] Zhou P, Wu C. Numerical study on the compression effect of gas diffusion layer on PEMFC performance. J Power Sources 2007;170(1):93–100.
[24] Mehboob H, Kyun PM, An-Soo K, Zai BA, Ali R. Analysis of the clamping pressure effect in PEM fuel cell structure by FEM and experiment. In: Third European Fuel Cell Technology & Application Piero Lunghi Conference; 2009.
[25] Ul Hassan N, Kilic M, Okumus E, Tunaboylu B, Murat Soydan A. Experimental determination of optimal clamping torque for AB-PEM fuel cell. J Electrochem Sci Eng 2016;6(1):9–16.
[26] Siracusano S, Di Blasi A, Baglio V, Brunaccini G, Briguglio N, Stassi A, et al. Optimization of components and assembling in a PEM electrolyzer stack. Int J Hydrogen Energy 2011;36(5):3333–9.
[27] Selamet ÖF, Becerikli F, Mat MD, Kaplan Y. Development and testing of a highly efficient proton exchange membrane (PEM) electrolyzer stack. Int J Hydrogen Energy 2011;36(17):11480–7.
[28] Selamet ÖF, Acar MC, Mat MD, Kaplan Y. Effects of operating parameters on the performance of a high-pressure proton exchange membrane electrolyzer. Int J Energy Res 2013;37(5):457–67.
[29] Selamet OF, Ergoktas MS. Effects of bolt torque and contact resistance on the performance of the polymer electrolyte membrane electrolyzers. J Power Sources 2015;281:103–13.
[30] Awasthi A, Scott K, Basu S. Dynamic modeling and simulation of a proton exchange membrane electrolyzer for hydrogen production. Int J Hydrogen Energy 2011;36(22):14779–86.
[31] Marangio F, Santarelli M, Cali M. Theoretical model and experimental analysis of a high pressure PEM water electrolyser for hydrogen production. Int J Hydrogen Energy 2009;34(3):1143–58.
[32] Al Shakhshir S, Frensch S, Kær SK. On the Experimental Investigation of the Clamping Pressure Effects on the Proton Exchange Membrane Water Electrolyser Cell Performance. In: Meeting Abstracts (No. 31, pp. 1515–1515). The Electrochemical Society.
[33] Debe MK, Hendricks SM, Vernstrom GD, Meyers M, Brostrom M, Stephens M, et al. Initial performance and durability of ultra-low loaded NSTF electrodes for PEM electrolyzers. J Electrochem Soc 2012;159(6):K165–76.
[34] Baik KD, Hong BK, Kim MS. Effects of operating parameters on hydrogen crossover rate through Nafion® membranes in polymer electrolyte membrane fuel cells. Renew Energy 2013;57:234–9.
[35] Baik KD, Kim MS. Characterization of nitrogen gas crossover through the membrane in proton-exchange membrane fuel cells. Int J Hydrogen Energy 2011;36(1):732–9.
[36] Schalenbach M, Hoeh MA, Gostick JT, Lueke W, Stolten D. Gas permeation through Nafion. Part 2: resistor network model. J Phys Chem C 2015;119(45):25156–69.
[37] Zhang J, Tang Y, Song C, Zhang J, Wang H. PEM fuel cell open circuit voltage (OCV) in the temperature range of 23 C to 120 C. J Power Sources 2006;163(1):532–7.
[38] LaConti A, Fragala A, Boyack J. Solid polymer electrolyte electrochemical cells-Electrode and other materials considerations. In: Symposium on electrode materials and processes for energy conversion and storage; 1977.
[39] Jung A, Oh J, Han K, Kim MS. An experimental study on the hydrogen crossover in polymer electrolyte membrane fuel cells for various current densities. Appl Energy 2016;175:212–7.
[40] Bessarabov D, Kruger A, Luopa SM, Park J, Molnar AA, Lewinski KA. Gas crossover mitigation in PEM water electrolysis: hydrogen cross-over benchmark study of 3M's Ir-NSTF based electrolysis catalyst-coated membranes. ECS Trans 2016;75(14):1165–73.
[41] Stern S. The "Barrer" permeability unit. J Polym Sci Part A-2 Polym Phys 1968;6(11):1933–4.
[42] Grigoriev SA, Porembskiy VI, Korobtsev SV, Fateev VN, Auprêtre F, Millet P. High-pressure PEM water electrolysis and corresponding safety issues. Int J Hydrogen Energy 2011;36(3):2721–8.
[43] Inaba M, Kinumoto T, Kiriake M, Umebayashi R, Tasaka A, Ogumi Z. Gas crossover and membrane degradation in polymer electrolyte fuel cells. Electrochim Acta 2006;51(26):5746–53.
[44] Schalenbach M, Hoefner T, Paciok P, Carmo M, Lueke W, Stolten D. Gas permeation through Nafion. Part 1: measurements. J Phys Chem C 2015;119(45):25145–55.